Bioactive Materials 25 (2023) 387–398

Contents lists available at ScienceDirect

Bioactive Materials

journal homepage: www.keaipublishing.com/en/journals/bioactive-materials

In utero delivery of mRNA to the heart, diaphragm and muscle with lipid nanoparticles

Kewa Gao [a,c,1], Jie Li [b,1], Hengyue Song [a,c,e], Hesong Han [b], Yongheng Wang [a,c,d], Boyan Yin [a,c], Diana L. Farmer [a,c], Niren Murthy [b,**], Aijun Wang [a,c,d,*]

[a] Department of Surgery, School of Medicine, University of California, Davis, Sacramento, CA, 95817, United States
[b] Department of Bioengineering, University of California, Berkeley, CA, 94704, United States
[c] Institute for Pediatric Regenerative Medicine, Shriners Hospitals for Children, Sacramento, CA, 95817, United States
[d] Department of Biomedical Engineering, University of California, Davis, CA, 95616, United States
[e] Department of Burns and Plastic Surgery, The Third Xiangya Hospital of Central South University, Hunan, 410013, China

ARTICLE INFO

Keywords:
In utero
mRNA delivery
Nanoparticles
Gene editing
CRISPR/Cas9

ABSTRACT

Nanoparticle-based drug delivery systems have the potential to revolutionize medicine, but their low vascular permeability and rapid clearance by phagocytic cells have limited their medical impact. Nanoparticles delivered at the *in utero* stage can overcome these key limitations due to the high rate of angiogenesis and cell division in fetal tissue and the under-developed immune system. However, very little is known about nanoparticle drug delivery at the fetal stage of development. In this report, using Ai9 CRE reporter mice, we demonstrate that lipid nanoparticle (LNP) mRNA complexes can deliver mRNA *in utero*, and can access and transfect major organs, such as the heart, the liver, kidneys, lungs and the gastrointestinal tract with remarkable efficiency and low toxicity. In addition, at 4 weeks after birth, we demonstrate that 50.99 ± 5.05%, 36.62 ± 3.42% and 23.7 ± 3.21% of myofiber in the diaphragm, heart and skeletal muscle, respectively, were transfected. Finally, we show here that Cas9 mRNA and sgRNA complexed to LNPs were able to edit the fetal organs *in utero*. These experiments demonstrate the possibility of non-viral delivery of mRNA to organs outside of the liver *in utero*, which provides a promising strategy for treating a wide variety of devastating diseases before birth.

1. Introduction

Developmental disorders, such as Duchenne muscular dystrophy, cerebral palsy, Fragile X syndrome and numerous others, cause devastating outcomes, affect millions of babies each year, and cause tremendous economic and emotional burdens to society [1–3]. Advances in prenatal genetic screening, imaging and our understanding of the molecular biology of fetal diseases have made it possible to diagnose numerous fetal diseases before permanent damage to the child has occurred. However, despite these advances, most fetal diseases remain untreatable due to a lack of tools and effective therapeutics.

The delivery of mRNA *in utero* via lipid nanoparticles (LNPs) has tremendous potential for treating fetal diseases. mRNA based therapeutics are highly modular and can be easily engineered to deliver a wide variety of therapeutic proteins ranging from intracellular proteins, gene editing enzymes and secreted proteins, which collectively have the potential to treat a wide variety of fetal diseases [4–8]. In addition, mRNA-based therapeutics have an excellent clinical track record and can be manufactured on a cost-effective scale, thus making their translation for treating a wide range of fetal diseases economically viable for companies interested in pursuing mRNA based fetal therapeutics [9].

Treating developmental diseases with mRNA/LNP complexes at the fetal stage may also be more efficacious and cost-effective than treatment after birth, due to the small cell number present in the developing fetus. For example, a human fetus in the second trimester, a gestational

Peer review under responsibility of KeAi Communications Co., Ltd.
* Corresponding author. Center for Surgical Bioengineering, Department of Surgery, School of Medicine, University of California, Davis, Sacramento, CA, 95817, United States.
** Corresponding author. Department of Bioengineering, University of California, Berkeley, CA, 94704, United States.
E-mail addresses: nmurthy@berkeley.edu (N. Murthy), aawang@ucdavis.edu (A. Wang).
[1] These authors contributed equally to the study.

https://doi.org/10.1016/j.bioactmat.2023.02.011
Received 24 October 2022; Received in revised form 26 January 2023; Accepted 11 February 2023

age at which *in utero* treatment is technically feasible, is about 1% the weight of a 1-year-old child [10]. In addition, the fetal immune system is tolerogenic and may not generate an immune response against foreign proteins and immunostimulatory nanoparticles, which is a frequent problem in adults [4,10]. Additionally, stem and progenitor cells are prevalent in the developing fetus and often actively proliferate, which may facilitate more efficient mRNA transfection [11,12]. Moreover, the biological barriers associated with blood vessel permeability may not be present, and phagocytosis is premature at the developing fetal stage, therefore systemically applied nanoparticle-based reagents have the potential to transfect multiple organs such as the liver, heart, skin, GI tract and brain at the *in utero* stage [4,5,13,14]. In addition, *in utero* injections can be performed safely, at low cost, without sophisticated infrastructure, allowing it to be utilized in all parts of the world, including economically under-developed regions [11]. Therefore, *in utero* delivery of mRNA/LNP complexes has the potential to significantly impact the treatment of developmental fetal diseases.

LNPs are a powerful methodology for the delivery of mRNA *in vivo* [15]. However, LNP delivery *in utero* has not been extensively studied. The feasibility of delivering mRNA *in utero* has recently been demonstrated by Riley et al., where they showed that an intravascular delivery of LNP mRNA complexes could transfect cells in the liver with an efficiency of approximately 1% [12]. These pioneering studies have demonstrated that LNPs containing GFP mRNA are well tolerated *in utero* after intravascular delivery. However, the cell types transfected with LNP/mRNA complexes *in utero*, and the long-term cell fate and mapping to adult tissues are still unclear. In addition, the effects of administering LNP/mRNA complexes via different routes of administration and delivery of LNP mRNA complexes at different gestational stages have not been investigated. These gaps in our understanding of *in utero* mRNA delivery have hindered the development of mRNA-based *in utero* therapeutics.

In this report, using Ai9 CRE reporter mice, we demonstrate that mRNA/LNP complexes can deliver mRNA *in utero*, and can transfect major organs, such as the liver, the heart, kidneys, lungs, GI tract and brain, with remarkable efficiency. We show here that CRE mRNA complexed to LNPs were able to transfect Ai9 mice *in utero* after the injection and transfected 0.64–12.4% of the cells in the heart, lungs, liver, kidneys, GI tract and brain, with low toxicity. In addition, the mRNA/LNP complex showed tropism to muscle tissues, and we found that a large number of myogenic stem cells were transfected in the heart, diaphragm and skeletal muscle. At 4 weeks after birth, we demonstrate that 50.99 $\pm$ 5.05%, 36.62 $\pm$ 3.42% and 23.7 $\pm$ 3.21% of myofibers in the diaphragm, heart and skeletal muscle were transfected, respectively. In addition, Cas9 mRNA and sgRNA complexed to LNPs were also able to edit Ai9 mice *in utero*, and edited 0.2–0.8% of cells in the liver, heart, GI, and kidneys. These experiments demonstrate the promise of using mRNA/LNP complexes for treatment of a wide range of fetal diseases related to these organs.

2. Results and discussion

2.1. Scientific rationale for in utero delivery of LNP/mRNA complexes

Delivering mRNA by nanoparticles to organs outside of the liver is a major challenge in adults due to the lower permeability of the vasculature, the large diffusion distances and the rapid phagocytic clearance of nanoparticles [16,17]. The *in utero* environment is drastically different from the adult environment and may offer unique opportunities for nanoparticle drug delivery. In particular, endothelial cells are undergoing significant levels of angiogenesis in all organs *in utero*, and there is consequently a great potential for large increases in permeability. Angiogenesis rarely occurs in adults, except in tumors, and nanoparticle drug delivery to tumors has been particularly successful. Similarly, the *in utero* environment may have lower numbers of mature macrophages, and consequently, the circulation half-life of nanoparticles may also be significantly extended.

However, despite its promise, very little is known about *in utero* mRNA delivery thus far. mRNA/LNP complexes have been investigated via intravascular delivery in a murine model with moderate success, resulting in 1% of liver cells being transfected [12]. Developing effective transfection approaches to achieve clinically meaningful mRNA delivery rates are therefore greatly needed.

Intrahepatic injection is well established as an effective approach to obtain direct vascular access *in utero*, and can be easily translated to intravenous umbilical cord injection under ultrasound guidance for human patients in clinical settings [18,19]. Compared to reported intravascular delivery in mice, intrahepatic delivery can be carried out at an earlier gestational stage, and this may lead to substantial differences in the overall transfection efficacy as well as in the types of cells transfected [18–20].

2.2. Characterization of LNPs and in vitro mRNA delivery efficiency in NIH 3T3 CRE reporter cells

LNPs have been widely used for the delivery of siRNA and mRNA to treat adult diseases [21,22]. In particular, LNP formulations based upon D-Lin, DSPC, cholesterol and PEG-DMG have been widely used for siRNA delivery and are the essential components of the first FDA approved siRNA drug Onpattro [22]. D-Lin containing LNPs have been delivered via the intravenous route, *in utero*, with moderate success, however, the potential of D-Lin containing LNP formulations for *in utero* treatment applications fetal therapy has not been fully investigated. Here we developed 4 different LNPs using D-Lin as the ionizable lipid components to explore their potential to deliver RNAs *in utero*. D-Lin containing LNPs were formed using the ethanol dilution method [23] by rapid mixing of lipid mixtures containing ionizable lipid (D-Lin-MC3-DMA), DOPE, cholesterol and PEG-lipids in the ethanol phase with mRNA in the aqueous phase. D-Lin enables mRNA encapsulation, cellular uptake and endosomal escape of the encapsulated mRNA into the cytosol [24], while DOPE and cholesterol provide stability of LNPs and may assist in endosomal escape [25,26]. The PEG-lipids enhance overall LNP stability and extend circulation times [27]. Four different cationic lipid formulations and lipofectamine were screened (see Table 1 for details of formulations). LNPs were characterized by size and mRNA encapsulation efficiency (Table S1). The hydrodynamic diameter, as assessed by dynamic light scattering (DLS) for all LNP formulations, ranged from 112.5 to 144.0 nm with PDI values less than 0.15, indicating monodisperse LNPs. Each LNP formulation was evaluated for its ability to encapsulate mRNA by RiboGreen assays [28], and all encapsulation efficiencies were high, ranging from 74.6 to 82.9%. The LNPs containing CRE mRNA exhibited high delivery efficiency in NIH 3T3 CRE reporter cells via flow cytometry measurement of transfected td-Tomato positive cells. LNPs treated cells showed high mRNA delivery efficiency with td-Tomato positive rate ranging from 53.2% to 61.8%, which is at least 66% increase compared with cells treated with mRNA/lipofectamine 2000 complexes (Fig. S1). The good mRNA encapsulation efficiency, excellent size distribution and *in vitro* mRNA delivery efficiency of these LNPs indicate they are good candidates for *in utero* therapy.

Table 1
Detailed formulation components of LNPs 1–4.

	LNP1	LNP2	LNP3	LNP4
D-Lin-MC3-DMA	36.8%	45.4%	38.3%	35%
DOPE	23.8%	15.7%	11.0%	16%
Cholesterol	38.2%	37.7%	49.5%	46.5%
DMG-PEG2000	1.2%	1.2%	1.2%	2.5%

2.3. LNPs can distribute to various internal organs after in utero delivery

A key challenge with using nanoparticles for drug delivery is their rapid clearance by the liver and their low vascular permeability (see Fig. 1). However, it is unknown if the *in utero* environment will be similarly challenging for nanoparticle drug delivery. Therefore, we performed experiments to determine the biodistribution of LNPs injected intrahepatically at the gestational age of E15.5 and compared their biodistribution with LNPs injected in adult mice. We chose E15.5 pregnant mice in this study mainly because its clinical correlation to the fetal treatment of human embryos. It has been well documented that mouse E15-16 pregnancy is equivalent to human 65–84 days of pregnancy on the basis of the development of the embryological structures [29]. Mouse E15.5 is approximately the earliest and most effective time point in mice that is equivalent to the timeline of prenatal diagnosis and treatment in humans. For these experiments, we used LNPs that contained Cy7 labeled PEG-Lipid and CRE mRNA. Specifically, blue food dye was added to make the injection position visible through the maternal uterus wall and fetal abdominal wall. The blue reagent gathered in the fetal liver right after injection, and then spread throughout the whole fetus with the blood circulation (see surgery procedure in Fig. 2B), demonstrating that our injection was successfully delivered into the fetal liver. Saline was injected into fetuses via the same route as LNPs to serve as a negative control.

Fig. 2C and D demonstrate that LNPs are distributed into several internal organs after an *in utero* delivery, 3 h post injection, and gradually increased over time. The Cy7 signal was evenly distributed in the heart, lungs, the liver, kidneys, the GI tract and the brain, suggesting that the LNPs access and persist in circulation for several hours. The proportion of cells that took up Cy7 labeled LNPs in each organ was quantified by flow cytometry. Age-matched mice injected with saline served as negative controls to gate the positive cell populations. The heart and liver revealed the highest uptake rate of injected LNPs at 24 h post injection, which were 5.49 ± 2.02% and 5.31 ± 1.20% positive for LNPs, respectively (Fig. 2E). These results demonstrate that the intrahepatically injected LNPs were not immediately taken up by the liver, and quickly entered the circulation and reached all parts of the body. The percentage of Cy7 positive cells was highest in the heart and liver, presumably due to their rich blood supply during the fetal period. The difference in organ distribution may also be closely related to the stage of organ development. The hepatocytes and immune cells in the fetus are still developing and not functionally mature, which may allow LNPs to reach extrahepatic organs before being cleared as we would see in adult animals. Additionally, the heart and the brain are the earliest organs of embryonic development, which may allow these organs to have greater exposure to LNPs relative to other organs that are still in the early stages of development. These have been well reported in the literature, for example it has been reported that the heart has completed the development of the 4-chambered structure and has a rich blood supply before E17 [30,31]. While at this stage, other organs are still at the beginning of the development.

The biodistribution of LNPs injected into the developing fetus was significantly different from adult animals. The Cy7-labeled LNPs injected during adulthood were exclusively taken up by the liver, 24 h post injection. This is consistent with numerous studies demonstrating that LNPs injected during adulthood are mainly captured by macrophages and hepatocytes in the liver [32] and have low efficiency of extrahepatic uptake. In contrast, the unique development of fetal organs during the

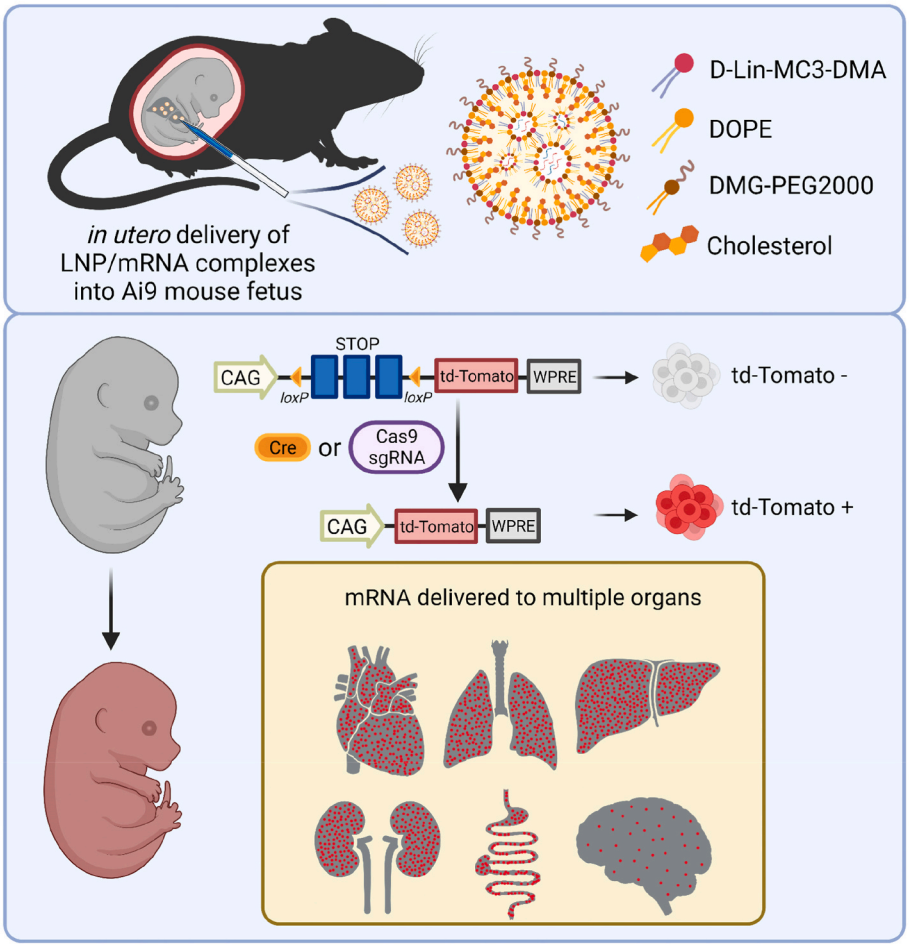

Fig. 1. LNPs can deliver mRNA *in utero* and efficiently transfect the heart, lungs, kidneys, the liver and the GI tract. In this report we demonstrate that lipid nanoparticle (LNP) mRNA complexes can deliver mRNA *in utero*, and can access and edit major organs, such as the heart, the liver, kidneys, lungs and the gastrointestinal tract with remarkable efficiency. These experiments demonstrate that mRNA can be delivered *in utero* via non-viral delivery methods and provide a strategy for treating a wide variety of fetal diseases.

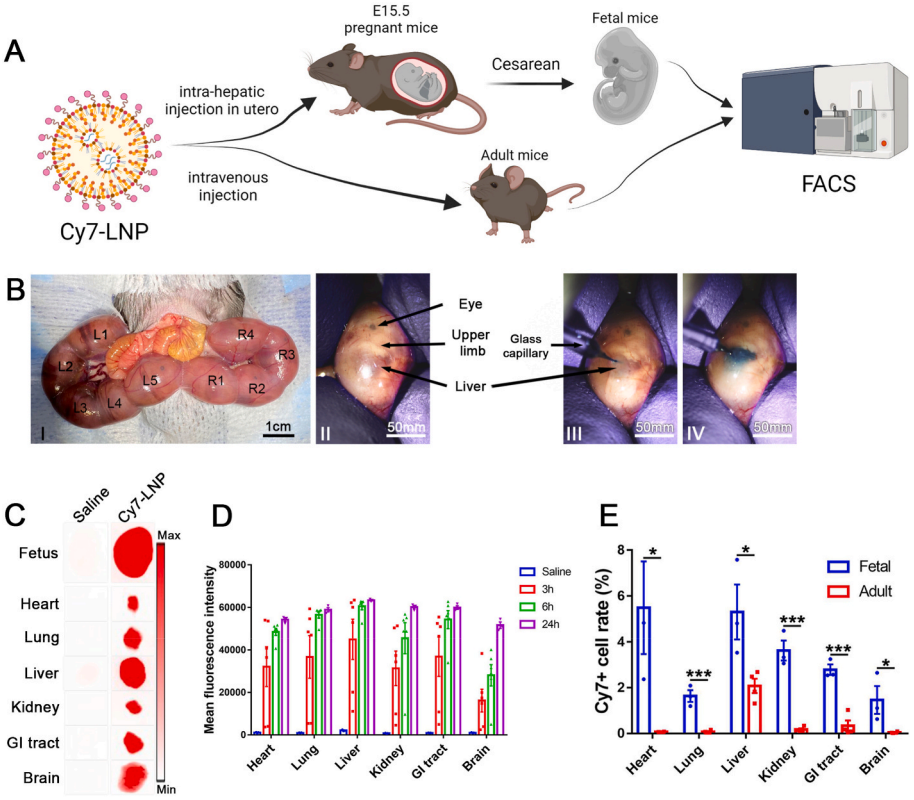

Fig. 2. LNPs injected *in utero* are permeable to the vasculature and can distribute to various internal organs. (A) Schematic depicting biodistribution experiments of Cy7 labeled LNP1. (B) Intraoperative photography of the *in utero* intrahepatic injection procedure. (I). The uterus of the pregnant mouse was exposed. (II). Identify the location of the fetal liver. (III). Puncture the fetal liver with a glass capillary. (IV). LNP1 labeled with food dye was injected into the fetal liver. (C) Cy7 labeled LNP1 was imaged in the whole E15.5 mouse fetus and internal organs after *in utero* injection demonstrate that LNP1 can distribute into multiple organs at 24 h post injection. (D) Quantitative analysis of the fluorescence intensity of Cy7 labeled LNP1. Cy7 signals can already be detected in various organs 3 h post injection and gradually increase as time increases (Data are represented as mean ± SEM, n = 6). (E) The Cy7 uptake rates post *in utero* injection were measured by flow cytometry and compared to adulthood injection. LNP1 injected during adulthood is mainly captured by cells in the liver. In contrast, LNP1 injected during the fetal period can reach various internal organs after 24 h post injection. The uptake rates of LNP1 injected during the fetal period was significantly higher than that of LNP1 injected during the adult period. (Data are represented as mean ± SEM, n = 3, *p < 0.05, ***p < 0.0001).

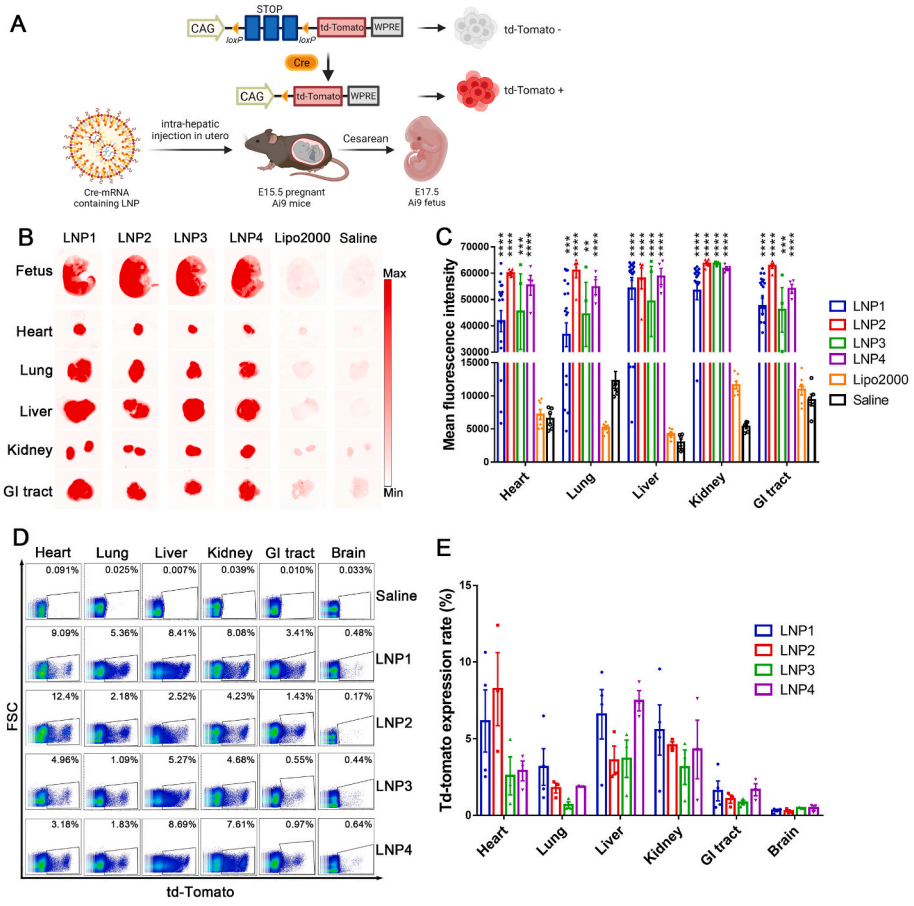

Fig. 3. LNPs containing CRE mRNA can transfect the heart, lung, kidney, liver and GI tract *in utero*. (A) Schematic describing transfection of Ai9 mouse fetuses with CRE mRNA delivered by LNPs 1–4. (B) Whole fetus and internal organ imaging of the transfected mice demonstrate that LNP 1–4 containing D-Lin can efficiently transfect multiple organs at 48 h post-injection. In particular, lungs, the liver, kidneys, the heart and the GI tract were all efficiently transfected. Lipofectamine was not effective after *in utero* injection. (C) Quantitative analysis of the fluorescence observed in B. LNPs were much more efficient at mRNA delivery than lipofectamine (Data are represented as mean ± SEM, n = 20 for LNP1, n = 5 for LNP2, n = 4 for LNP3, n = 4 for LNP4, n = 7 for Lipo2000). Saline served as a control (n = 6). All four LNP formulations transfected multiple organs. (D) Flow cytometry analysis of *in utero* transfected organs. (E) Quantitative analysis of D. Greater than 1% transfection was observed in a variety of organs. Approximately 5–10% of the cells in the liver, heart and kidney, and 3–4% of the cells in the lung and GI tract were transduced. (Data are represented as mean ± SEM, n = 3).

gestational period [33] allows LNPs delivered at the *in utero* stage to persist in circulation for an extended period and transfect internal organs other than the liver. These results highlight that the fetal period may serve as a unique window for the treatment of diseases involving non-liver organs.

2.4. LNPs can deliver CRE mRNA and transfect a wide variety of tissues *in utero*

The biodistribution studies performed above suggest that *in utero* administration of LNPs has the potential to deliver macromolecules to organs outside of the liver. We, therefore, performed experiments to determine if *in utero* injection of mRNA/LNP formulations could transfect mRNA *in utero*, and also identified the cell types and organs transfected. We used Ai9 CRE reporter mice for these experiments to test the CRE mRNA delivery efficiency. This combination was chosen because it generates a permanent td-Tomato expression in cells that received the mRNA, which allows for the identification of the transfected cell types. Four different cationic lipid formulations and lipofectamine were screened (see Table 1 for details of formulations) and were injected *in utero* at the gestational age of E15.5 and then analyzed 48 h later via whole fetus and organ imaging. The four LNP based formulations contained various ratios of ionizable lipid D-Lin, DOPE, cholesterol and DMG-PEG2000, and were selected because of their ability to efficiently deliver mRNA in adult mice [23].

Fig. 3B demonstrates that LNPs containing D-Lin were remarkably effective at transfecting mRNA *in utero*, compared to commercially available lipofectamine 2000, which was not effective at transfecting fetal organs and was not investigated further. All four LNP formulations containing D-Lin were able to transfect several organs after the injection. In particular, the heart, lungs, the liver, kidneys and the GI tract were td-Tomato positive after injection with LNPs containing D-Lin (Fig. 3B and C). The broad tissue distribution of CRE mRNA delivery after the injection suggests that the fetal environment is permeable to nanoparticles, where the nanoparticles are able to enter a variety of vasculature and then transfect a variety of tissues. *In utero* delivery gave a much broader tissue distribution and transfection of CRE mRNA than in adult mice. The *in utero* transfection levels *in utero* were similar between the heart, lungs, the liver, kidneys, the GI tract, presumably due to simultaneous diffusion into the vasculature of multiple organs. In contrast, the delivery of LNPs in adults generates transfection predominantly in the liver [34]. The ability to transfect organs such as the heart and kidneys is significant as these organs are the targets for a variety of fetal diseases and have been challenging to transfect with mRNA, due to the low permeability of their vasculature. *In utero* delivery of mRNA/LNP complexes has the potential to create a variety of new therapeutic strategies for fetal diseases.

2.5. LNPs are efficient at delivering mRNA in utero

The percentage of cells transfected after *in utero* delivery of mRNA/LNP complexes is a key parameter that will determine the clinical potential of this delivery strategy. We consequently determined the mRNA delivery efficiency of mRNA/LNP complexes containing CRE mRNA. Ai9 mice were treated as described above, and after 48 h the organs were harvested, digested and analyzed by flow cytometry to determine the percentage of cells that were transfected in each organ. Fig. 3D and E demonstrate that an intrahepatic injection of mRNA/LNP complexes is efficient at delivering CRE mRNA. For example, more than 1% of the cells in the heart, lungs, the liver, kidneys, and the GI tract were transfected using the intrahepatic delivery route, which appears to have a higher efficiency than the *in utero* intravascular route of administration. To illustrate, Riley et al. demonstrated that *in utero* injection of mRNA/LNP complexes via the vitelline vein resulted in 1% of cells in the liver being transfected with GFP [12]. In contrast, intrahepatic injection of LNPs transfected approximately 5–10% of the cells in the liver, heart and kidney, and 3–4% of the cells in the lung and GI tract in the Ai9 mouse model (Fig. 3D and E). The blood-brain barrier (BBB) has probably partially developed and has certain effects even in the fetal period which may explain why the transfection rate of the brain was lower than other organs. The main function of the BBB is to block the entry of biological macromolecules, including mRNAs, into the brain [35]. In humans, the BBB development begins in the early embryo and matures before 31 weeks of gestation [36]. The mouse BBB was reported to become functional at E15.5 [37]. The difference between the Cy7 uptake and mRNA transfection indicates that the BBB was partially functional at this stage. Overall, it is important to note that the vast majority of these organs have been impossible to transfect in adult animals, and *in utero* mRNA delivery appears to provide a robust methodology for accomplishing this [4,5,11].

We further investigated the cell type of transfected cells after *in utero* delivery by immunohistochemistry staining. The phenotype of mRNA/LNP1 complexes transfected and td-Tomato expressing cells in the heart (Fig. 4-c,f,i), diaphragm (Fig. 4-d,g,j) and skeletal muscle (Fig. 4-e,h,k) were characterized by IHC, staining for Pax7 a primitive myogenic marker [38], and myogenin a transcriptional regulatory protein involved in skeletal muscle differentiation [39]. A large number of td-Tomato positive cells were found in the heart, diaphragm and skeletal muscle. In addition, staining with the proliferation marker cyclin A, demonstrated a wide distribution of proliferating cells that were also td-Tomato positive (Fig. 4-i,j,k), which represents muscle stem cells (MuSCs) that are actively dividing and will proliferate and differentiate into myofibers as the fetus develops. The mRNA/LNP2-4 complexes showed equivalent ability to transduce MuSCs in the heart, diaphragm and skeletal muscle as evidenced by td-Tomato expressing cells in these organs (Figs. S2–4).

2.6. In utero injection of CRE mRNA/LNP1 results in no obvious toxicity to internal organs and has minimal effects on inflammatory cytokine expression levels

We next determined the toxicity of CRE mRNA/LNP complexes to fetuses 48 h post injection. The fetuses showed good tolerance to *in utero* injection of LNPs. The survival rate of fetuses treated with mRNA/LNP complexes was 96.3% (LNPs 1–4), and close to the survival rate of saline injected fetuses (100%) (see Table S2). The morphology of the internal organs, the heart, lungs, the liver and kidneys were also evaluated by H&E staining. The morphology of the internal organs of mRNA/LNPs treated fetuses showed a normal structure (Fig. 5A upper panel and Fig. S6), similar to the saline treated fetuses (Fig. S5 upper panel), and was without obvious tissue liquefaction, atrophy, or necrosis. At the same time, a high mRNA delivery efficiency was achieved by this formulation. A large number of td-Tomato positive cells were observed in the internal organs and distributed evenly throughout the organ (Fig. 5A middle and lower panel). In addition, there were no td-Tomato positive cells in the saline treated fetuses (Fig. S5 middle and lower panel). Finally, we also examined the pregnant mother by histology, via H&E staining and td-Tomato expression, for evidence of toxicity and mRNA *trans*-placental delivery, after *in utero* injection with CRE mRNA/LNP1 complexes (see Figs. S7 and S8). We did not observe any signs of toxicity in the organs of the mother and 100% of the injected mothers survived (11/11 for CRE mRNA/LNP1), demonstrating that the mother tolerates *in utero* injections with CRE mRNA/LNP1 complexes. We also did not observe any td-Tomato positive cells in the mother, indicating that this intervention did not lead to maternal transfection.

We also measured the cytokine levels in the fetal liver after *in utero* injection with CRE mRNA/LNP1 to determine the inflammatory response triggered by LNP1 (see Fig. 5B). Fig. 5B demonstrates that CRE mRNA/LNP1 injections had a minimal impact on cytokine expression levels. In particular, 9/10 of the cytokines examined were statistically indistinguishable from the saline treated fetuses, including IFN-γ, IL-1β, IL-2, IL-4, IL-5, IL-6, IL-10, IL-12p70, TNF-α. The level of KC/GRO was

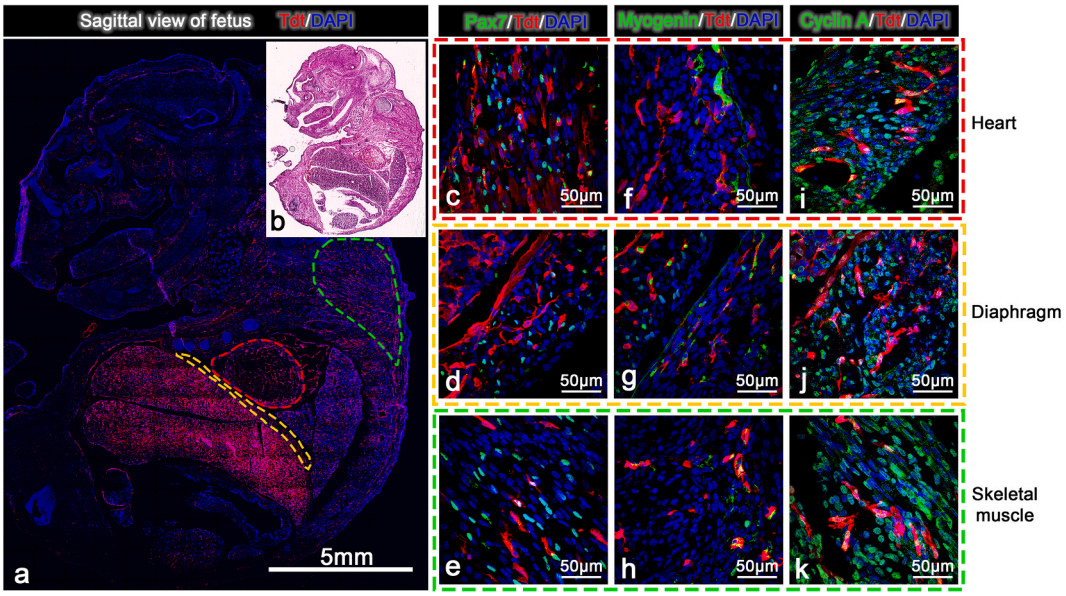

Fig. 4. ***In utero*** **delivery of CRE mRNA/LNPs can transfect large number of muscle stem cells in the heart, diaphragm and skeletal muscle.** Fluorescent imaging (a) and H&E staining (b) of td-Tomato expression in fetuses at 48 h after *in utero* injection of CRE mRNA/LNP1. Large numbers of td-Tomato expressing cells were detected in the heart, diaphragm and skeletal muscle. The phenotype of td-Tomato expressing cells in the heart (c,f,i), diaphragm (d,g,j) and skeletal muscle (e, h,k) were characterized by IHC. Transfected cells were positive for the muscle stem cell markers Pax7 (c,d,e) and myogenin (f,g,h) 48 h after injection. Transfected cells were also positive for the proliferation marker cyclin A (i,j,k).

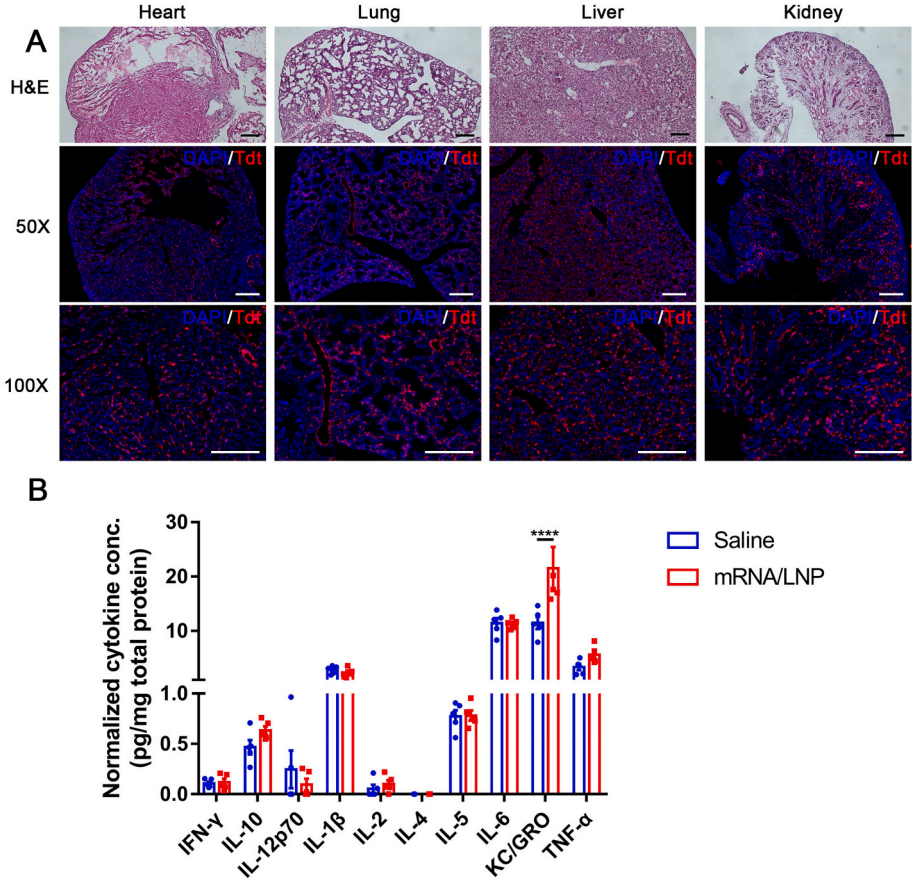

Fig. 5. ***In utero*** **injection of CRE mRNA/LNP1 results in no obvious toxicity to internal organs and has minimal effects on inflammatory cytokine expression.** (A) H&E staining and fluorescent imaging of td-Tomato expression in fetuses after *in utero* injection of CRE mRNA/LNP1. No signs of tissue damage or toxicity were observed via H&E staining in mRNA/LNP1 treated fetuses. td-Tomato expression was observed throughout the organs and was well distributed (Scale bar = 200 μm). (B) Cytokine analysis of the fetal liver, after *in utero* injection of mRNA/LNP1. Nine of the cytokines analyzed were statistically indistinguishable from the control saline injected mice. KC/GRO had a modest increase in expression (Data are represented as mean ± SEM, n = 5).

increased in LNP treated fetuses compared to saline control mice.

2.7. LNPs can transfect various cell types in the liver, the heart, lungs, kidneys and the GI tract with high efficiency

A key benefit of using the Ai9 mouse model is that cells transfected with CRE will permanently express td-Tomato and can consequently be identified via flow cytometry. Identifying the cell types transfected with mRNA/LNP formulations will provide valuable information with regard to the type of therapies that can be developed. LNP1 containing CRE mRNA was injected into Ai9 mouse fetuses as described above. The liver tissue was analyzed for mRNA delivery at different time points after injection. Forty-eight hours after injection, the mice were sacrificed, and the internal organ tissues were enzyme dissociated into single cells and stained with a panel of antibodies to determine the transfection rates in specific cell populations. Fig. 6A and Fig. S9 demonstrate that CD90$^+$ cells were the most efficiently transfected cell type in the developing liver, with 55.8 ± 2.52% of CD90$^+$ cells being transfected. In addition, other important cell types were also transfected, such as CD45$^+$ and CD71$^+$ cells, which are leukocytes and bone marrow progenitors. The transfection rate reached 12.1 ± 1.85% and 12.17 ± 1.5%, respectively. 34.5 ± 4.77% of cells with endothelial marker CD31$^+$, and 36.13 ± 2.31% of cells with the epithelial marker CD324$^+$ cells were transfected, which would be sufficient to develop treatments against a variety of diseases associated with these cells. The high level of endothelial cell transfection is presumably because the LNPs are being transported via the developing vasculature and these cells have access to the LNPs more readily than other cells. In adult mice, endothelial cells are difficult to transfect, particularly with LNPs [40]. However, the endothelial cells in the developing fetus should have substantial physiological differences from adult endothelial cells. In particular, they should have a higher rate of cell division and metabolism, and this may make them more phagocytic than adult endothelial cells. Endothelial cells are ideal targets for transfection with secreted proteins. The ability to efficiently transfect endothelial cells in the liver will open up numerous therapeutic applications.

LNPs were able to deliver mRNA to a variety of organs outside of the liver, and determining the cell types transfected in these organs will help identify the types of therapeutics that can be generated with *in utero* mRNA delivery. We studied the surface marker expression on the cells that were successfully transfected by mRNA/LNP complexes in the heart, lungs, kidneys and the GI tract to investigate the phenotypes of the transfected cells. The quantitative analyses are shown in Fig. 6 and representative flow cytometry figures are shown in the supplementary figures (Figs. S10–S13). The transfection rate of CD31$^+$ cells was the highest in the heart (33.27 ± 6.59%). While in the lungs, CD90$^+$ cells had the highest transfection rate at 43.1 ± 7.07%. In addition, CD31$^+$ cells also had a relatively high transfection rate (18.37 ± 3.82%) in the

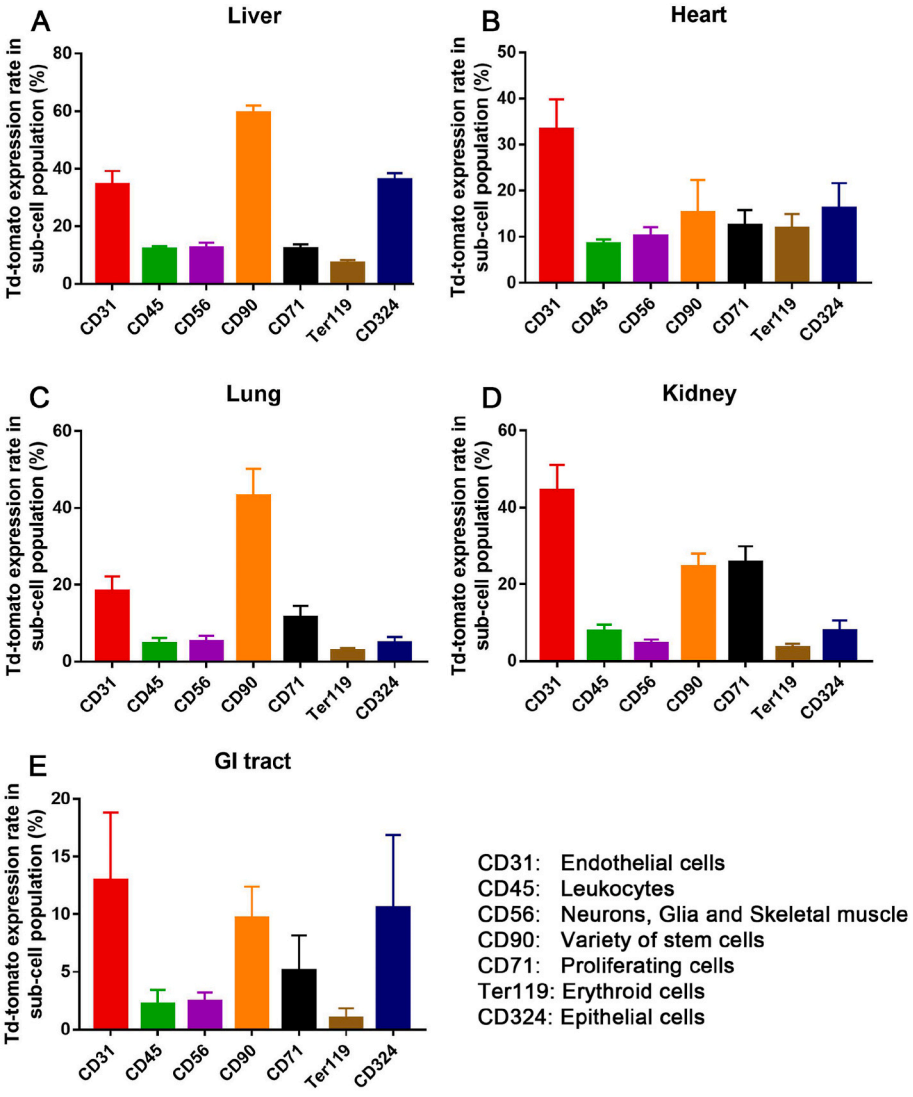

Fig. 6. CD31$^+$ and CD90$^+$ cells are efficiently transfected in the fetal heart, lung, liver, kidney and GI tract after an *in utero* injection of mRNA/LNP1 complexes. (A) Flow cytometry analysis of the transfection rate in specific cell populations of the liver after *in utero* injection of CRE mRNA/LNP1 complexes. 60% of CD90$^+$ cells were transfected and >30% of CD31$^+$ and CD324$^+$ cells were also transfected. (B) Cellular analysis of cells transfected in the heart. CD31$^+$ cells were transfected with an efficiency of 30% and a variety of other cell types were also transfected with an efficiency >5%. (C) Cellular analysis of cells transfected in the lung. CD90$^+$ cells were transfected with an efficiency of 40% and CD31$^+$ were also transfected with an efficiency of 20%. (D) Cellular analysis of cells transfected in the kidney. CD31$^+$ cells were transfected with an efficiency of 40%, CD90$^+$ and CD71$^+$ cells were also transfected with an efficiency of 20%. (E) Cellular analysis of cells transfected in the GI tract. CD31$^+$, CD90$^+$ and CD 324$^+$ cells were transfected with an efficiency of approximately 10%. (Data are represented as mean ± SEM, n = 3).

lungs. Similarly, in the kidney, $CD31^+$ cells were the most efficiently transfected cell type in the kidney (44.4 ± 6.61%), followed by $CD90^+$ cells (24.5 ± 3.52%) and $CD71^+$ cells (25.73 ± 4.19%).

2.8. Ai9 mice treated with CRE mRNA/LNP complexes have high levels of transfection in the heart and diaphragm in their progeny 4 weeks after birth

Since the cells will proliferate dramatically during fetal development, investigating the long-term fate of transfected cells after birth is of great interest. We performed a series of longitudinal studies in Ai9 mice treated with CRE mRNA *in utero*, to determine what cells were transfected after birth. In particular, we wanted to determine if the cells transfected *in utero* had a high proliferative capacity and had the potential to create mosaic organs with large numbers of transfected cells. Fig. 7 demonstrates that Ai9 mice treated with CRE mRNA/LNP1 complexes have large numbers of transfected cells in the heart and diaphragm at 4 weeks after birth in mice. We further stained the heart, diaphragm and skeletal muscle with the muscle specific antibodies desmin, myosin and laminin (Fig. 7) to determine if myofibers were being transfected. The immunostaining demonstrates that a large number of the transfected cells at the 4 weeks stage are $desmin^+$, $myosin^+$ or $laminin^+$ myofibers, suggesting that transfected MuSCs proliferate and differentiate during development. Laminin is a basal lamina protein that outlines individual myofibers and muscle sections are therefore routinely stained for Laminin to quantify the number and size of the myofibers [41]. In this study, the number of myofibers was counted from immunostaining of Laminin. The td-Tomato positive rate

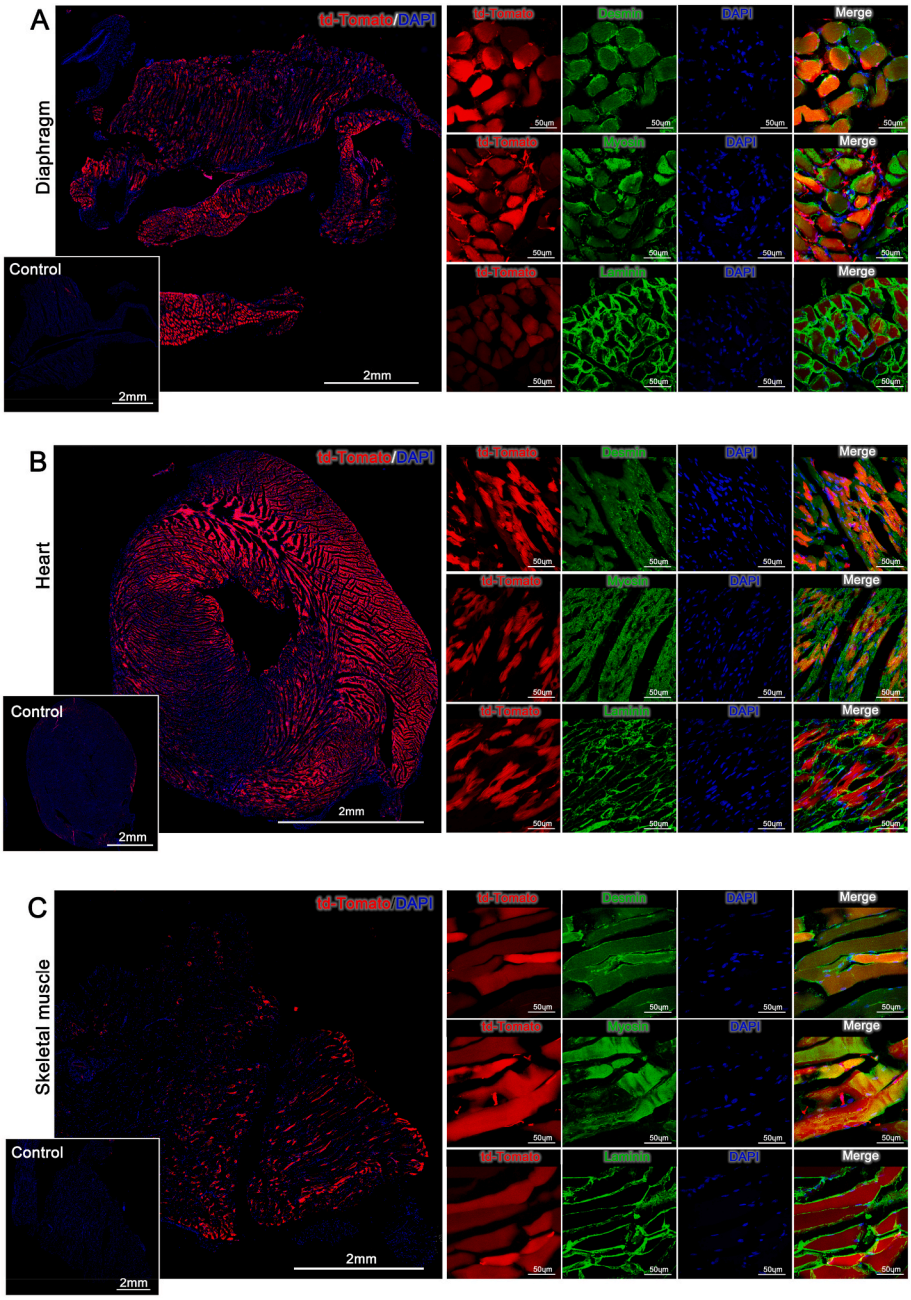

Fig. 7. Ai9 mice treated with CRE mRNA/LNP complexes have high levels of transfection in the heart and diaphragm in their progeny 4 weeks after birth. Immunohistochemistry staining images of the diaphragm (A), heart (B) and skeletal muscle (C). Desmin, Myosin and Laminin staining demonstrates that a large number of mature myofibers were transfected and expressed td-Tomato 4 weeks after birth.

of the myofibers is defined as the ratio of td-Tomato expressing myofibers in all Laminin$^+$ myofibers (td-Tomato$^+$/Laminin$^+$ myofibers). 50.99 ± 5.05%, 36.62 ± 3.42% and 23.7 ± 3.21% of the myofibers in the diaphragm, heart and skeletal muscle were respectively transfected (Fig. 8). However, CD31 and α-SMA staining showed that only a small number of transfected cells were derived from vascular structures (Figs. S14 and S15). The cell types of td-Tomato-positive cells at 48 h (Fig. 6B) and the 4-week (Fig. S14) after injection are significantly different, probably because muscle cells proliferate more robustly than endothelial cells. These experiments suggest that *in utero* mRNA delivery has great potential for treating devastating diseases such as muscular dystrophy and congenital heart disease.

2.9. LNPs can transfect Cas9 mRNA and edit internal organs of Ai9 mice

Having demonstrated that an *in utero* delivery of mRNA/LNP complexes was efficient at delivering CRE mRNA, we next sought to evaluate the editing efficiency of Cas9 mRNA/sgRNA. We performed *in utero* delivery of LNPs containing Cas9 mRNA/sgRNA into Ai9 mouse fetuses following the procedures described above. As described in Fig. 9A experimental scheme, the Cas9 mRNA/sgRNA transduction and genomic excision of the STOP cassette will subsequently activate the expression of td-Tomato. 48 h after *in utero* injection, the mice were sacrificed and the internal organs, including the heart, liver, lungs, kidneys, GI tract and brain were harvested, digested and analyzed by flow cytometry to determine the percentage of cells that were td-Tomato positive at 48 h post-injection. As shown in Fig. 9B and C, the Cas9-containing LNPs successfully led to td-Tomato expression in the kidney and liver of Ai9 mice after *in utero* delivery. The flow cytometry quantitative analysis in Fig. 8C shows that the editing efficiency of LNPs for kidneys and liver is above the baseline level of the control group, and LNP3 activated td-Tomato expression in 0.47 ± 0.14% (n = 5) of total kidney cells. These results demonstrate that mRNA/LNP complexes can be used to deliver CRISPR-Cas9 *in utero*. Compared to the CRE mRNA delivery, the Cas9 gene editing efficiency is relatively low. However, for many enzyme deficient diseases, therapeutic effects can be achieved even when editing rates are less than 1% [42]. Moreover, the percentage of edited cells may increase during fetal development due to the survival advantage and subsequent expansion of edited cells [43,44]. The *in utero* editing efficiency can be further improved by using modified sgRNAs and stabilizing the secondary structure of the sgRNA, as evidenced by studies in adult mice [45–47].

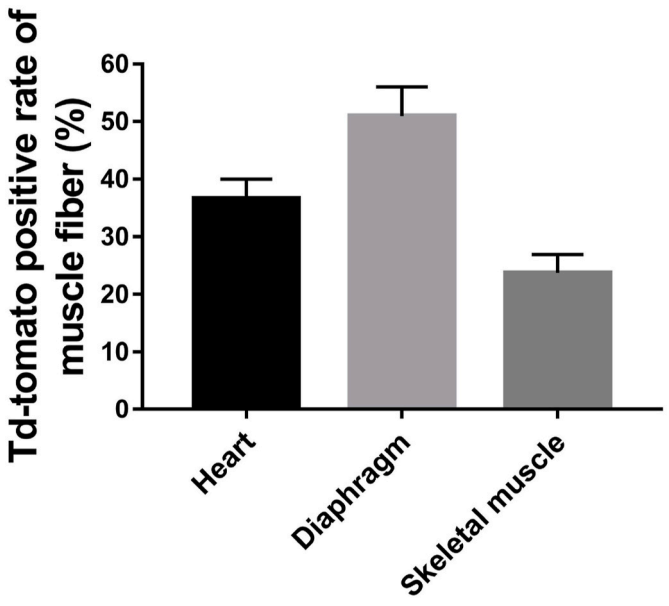

Fig. 8. The td-Tomato positive rate of myofibers was quantified by Laminin immunostaining shown in Fig. 7. (Data are represented as mean ± SEM, n = 4).

3. Conclusion

In this report, we demonstrate that LNPs containing the ionizable lipid D-Lin can deliver mRNA to a wide variety of organs and transfect non-phagocytic cells, such as CD45$^+$, CD31$^+$, CD90$^+$ and CD71$^+$ cells, via *in utero* injection. These cell types are almost impossible to transfect with nanoparticles in adult mice mainly due to the limited access to the vasculature. However, the *in utero* environment is characterized by intense levels of angiogenesis and cell division, both of which will increase the permeability of the vasculature and the endocytic activity of non-phagocytic cells. We observed more than 5% transfection levels with D-Lin based LNP formulations, and a wide variety of fetal diseases can potentially be treated with this level of mRNA delivery efficiency. However, the D-Lin LNP formulation was optimized for transfecting adult mice, therefore further optimization of LNP formulations for the *in utero* environment will likely lead to increased delivery efficiency, making their translation even more likely. In summary, *in utero* nanoparticle drug delivery has great potential for delivering macromolecules to organs outside of the liver and provides a promising strategy for treating a wide variety of devastating fetal diseases.

4. Methods

4.1. Materials

DLin-MC3-DMA was purchased from MedKoo Biosciences. DODAP, DODMA, DOPE, DMG-PEG (MW 2000) (DMG-PEG2000) and DSPE PEG (2000)-N-Cy7 were purchased from Avanti Polar Lipids. Cholesterol was purchased from Sigma Aldrich. Pur-A-Lyzer Midi Dialysis Kits (WMCO, 3.5 kDa) were purchased from Sigma. Cas9 mRNA and Cre mRNA were purchased from TriLink BioTechnologies. Modified sgAi9A, sgAi9B and sgAi9C (Table S3) were purchased from IDT.

4.2. Nanoparticle formation

RNA-loaded LNP formulations were formed using the ethanol dilution method [23]. All lipids with specified molar ratios (Table 1) were dissolved in ethanol and RNA was dissolved in a 10 mM citrate buffer (pH 4.0). The two solutions were rapidly mixed at an aqueous to ethanol ratio of 3/1 by volume (3/1, aq./ethanol, vol/vol) to satisfy a final weight ratio of 20/1 (total lipids/mRNA), then incubated for 10 min at room temperature. All formulations were named based on the additional lipids. The lipids molar ratio for LNP1-3 are D-Lin-MC3-DMA/DOPE/cholesterol/DMG-PEG ratio of 36.8/23.8/38.2/1.2, 45.4/15.7/37.7/1.2, 38.3/11.0/49.5/1.2 and the lipids molar ratio for LNP4 is 35/46.5/16/2.5, follows previous report for D-Lin formulation of mRNA [12]. For biodistribution studies, Cy7 labeled LNPs were used by substitute half of the DMG-PEG2000 in regular LNPs by DSPE PEG (2000)-N-Cy7 in terms of molar ratio. For Cas9/sgRNA, the weight ratio of Cas9 mRNA/sgAi9A/sgAi9B/sgAi9C is 2/0.2/0.2/0.6. After LNP formation, the fresh LNP formulations were diluted with Opti-MEM to 1.25 ng/μl mRNA (with a final ethanol concentration <0.2%) for *in vitro* assays and size detection using dynamic light scattering (Zetasizer Nano, Malvern). For RNA encapsulation efficacy was evaluated by the Ribogreen assay [28]. For *in vivo* experiments, the formulations were dialysed (Pur-A-Lyzer Midi Dialysis Kits, WMCO 3.5 kDa) against 1 × PBS for 2 h, and diluted with PBS to 0.125 μg/μl for *in utero* delivery.

4.3. Animal studies

All animal procedures were approved by The University of California, Davis (UCD) institutional animal care and use committee (IACUC). All facilities used during the study period were accredited by the

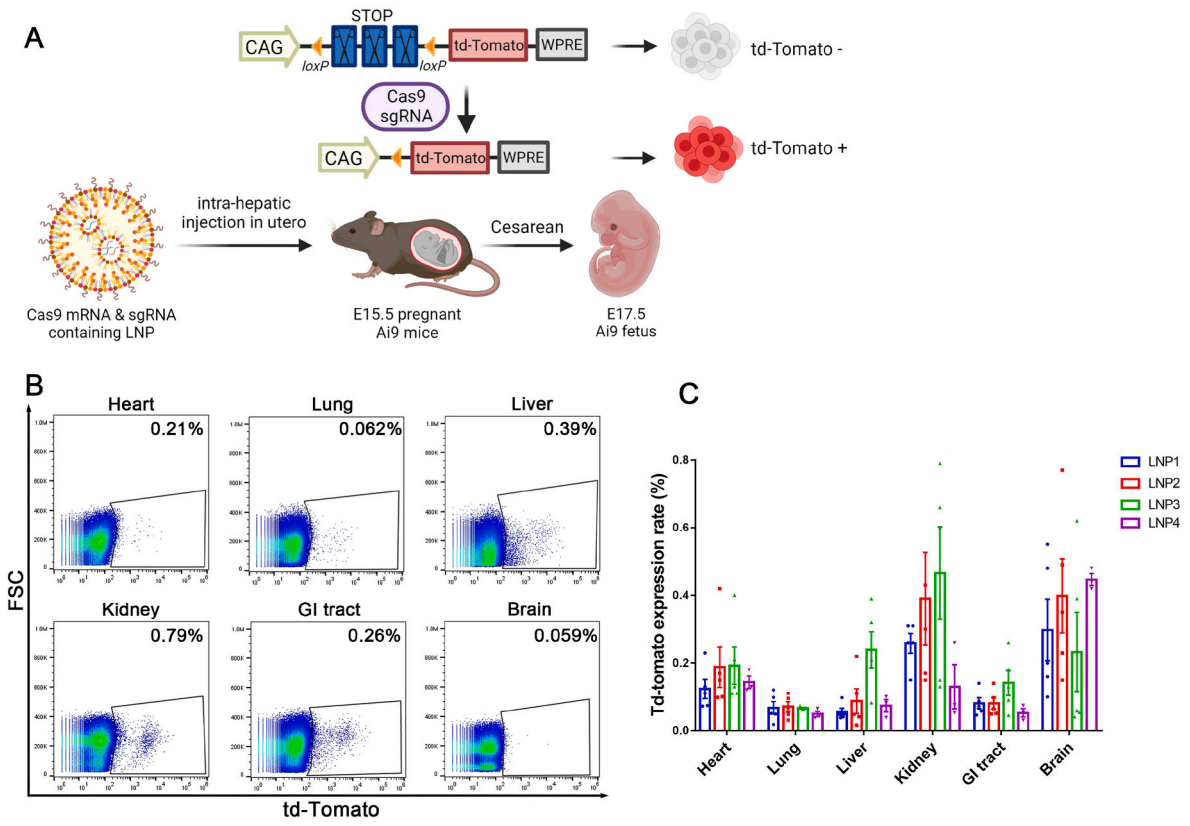

Fig. 9. mRNA complexed with LNPs 1–4 containing Cas9 mRNA can edit multiple internal organs after an *in utero* injection. (A) Schematic depicting the procedure of *in utero* Cas9 gene editing in the Ai9 mouse. (B) Flow cytometry of the various organs after transfection with Cas9mRNA/sgRNA/LNP3 complexes. The percent transfection of the various organs was determined. (C) Quantitative analysis of *in utero* editing with LNPs 1–4 in different organs. LNP3 is the most efficient formulation with regards to Cas9 mRNA delivery *in utero* and edited approximately 0.5% of the cells in the kidney. The liver was also transfected and 0.3% of the cells were transfected (Data are represented as mean ± SEM, n = 3).

Association for the Assessment and Accreditation of Laboratory Animal Care International (AAALAC). Ai9 transgenic mice were purchased from The Jackson Laboratory (Jackson stock No. 007909). Time-mated pregnant Ai9 mice (8–12 weeks old) were bred in-house at UCD and the *in utero* injections were performed as previously described [48]. At E15.5, the mouse was placed under isoflurane anesthesia (5% isoflurane for induction, 2% isoflurane for maintenance) and was positioned supine on a heating pad. A 2-cm midline laparotomy incision was performed and the uterus was carefully exteriorized with cotton applicators. The uterus was examined for the presence of fetuses and the number of normal and nonviable fetuses was noted (the uterus containing fetuses was shown in Fig. 2Bi). A glass pipette that had been pulled to a pore size of 70 μm was loaded with 5 μL of CRE mRNA or Cas9 mRNA containing LNPs were resuspended in PBS mixed with blue food coloring at a 1:10 ratio or saline as control. With the aid of a 10X operating microscope, the glass pipette was inserted through the uterus and fetal abdominal wall into the fetal liver. The blue food coloring allowed for visual confirmation of injected reagents located in the liver (Fig. 2B ii). The uterus was then returned to its original location in the abdomen and the maternal laparotomy was closed in 2 layers with absorbable 4-0 vicryl suture. The mouse then received a subcutaneous injection of 1 mL PBS for fluid resuscitation and a 0.05 mg/kg dose of buprenorphine for pain management. Mice after *in utero* injection were allowed to carry pregnancy for 48 h post-treatment and fetuses were delivered by c-section (E17.5). The survival of fetuses was assessed by observation of the size, skin color and spontaneous movement of the fetus. The fetuses and their dissected internal organs including the heart, the liver, lungs, kidneys, the GI tract and brain were imaged by ChemiDocTM MP imaging system (Bio-Rad, Hercules). To quantify the fluorescence density of the internal organs, regions of interest (ROIs) were drawn around the edge of organs and the average fluorescence densities were measured by ImageJ software.

4.4. Biodistribution

The biodistribution experiments were performed on Ai9 mouse fetuses at E15.5 and 12 weeks old adult Ai9 mice. Fetus mice were injected intrahepatically with 5ul of Cy7-labeled LNP1s as described above. 150ul of Cy7 labeled LNP1s were injected into adult mice from inner canthus. The same volume of saline without LNPs were injected as a control. Pregnant mice were euthanized at 3 h, 6 h and 24 h post LNP injection. Fetuses were delivered via cesarean section and washed in PBS. Internal organ including the heart, the liver, lungs, kidneys, the GI tract, and the brain were harvested and imaged by ChemiDocTM MP imaging system (Bio-Rad, Hercules). Adult mice were euthanized at 24 h post LNP injection. These mice were perfused with PBS to drain blood. Internal organs were harvested for flow cytometry analyses.

4.5. Flow cytometry

Flow cytometry was used to quantify the percentage of cells in organs that were Cy7 positive or td-Tomato positive following treatment. Single-cell suspensions were obtained as described previously [49,50] for further staining and flow cytometry analysis. Freshly dissected the heart, the liver, lungs, kidneys, the GI tract, and the brain were minced and digested with 500 μL of 1 mg/mL collagenase type I (Gibco) by incubating at 37 °C, 5% CO2 for 20 min in 1.5 ml Eppendorf tubes. Cell suspension was collected, neutralized with a medium containing 10% fetal bovine serum (FBS), and placed on ice. Fresh collagenase solution was added to the remaining tissue and incubated for an additional 20

min. Cell suspensions were filtered through 70um Nylon cell strainer (Falcon, cat. 352,350) to create a single-cell suspension. The Attune NxT Flow Cytometer (Thermo Fisher Scientific) was used for performing flow cytometry, and FlowJo software (FlowJo LLC) was used for data analyses. All antibodies were obtained from BD Biosciences. Cells were stained with BV421-CD56 (cat.748,094), APC-CD31 (551,262), FITC-CD90.2 (553,003), BV421-CD45 (563,890), BV650 CD324 (752, 472), FITC-CD71 (561,936), APC-Ter119 (557,909) from BD Biosciences. BDTM anti-Rat Ig, κ CompBeads (552,844) were used to generate compensation controls.

4.6. Histology and immunofluorescence staining

Fetal and maternal internal organs were fixed in 4% PFA for 24 h, dehydrated with 30% sucrose for 24 h, and embedded in the O.C.T compound (Sakura Finetek USA). Serial sections were made at the thickness of 10 μm using a Cryostat (Leica CM3050S) and collected onto microscope slides (Matsunami Glass). H&E staining was performed to characterize tissue morphology. Tissue sections were extensively washed with PBS, heat antigen retravel were performed within target retrieval solution, pH 9.0 (Dako). The sections were blocked with 5% BSA in PBS at room temperature for 1 h and stained with primary antibody at 4 °C overnight. The dilutions of primary antibodies were 1:100 for Desmin (abcam, ab32362), 1:200 for Myosin (Millipore Sigma, M1570), 1:100 for Laminin (Millipore Sigma, L9393), 1:100 for CD31 (Novus Biologicals, AF3628) and 1:200 for α-SMA (LSBio, LS-B3933), 1:10 for Pax7 (Developmental Studies Hybridoma Band), 1:100 for Cyclin A (Millipore Sigma, ZRB-1590), 1:50 for Myogenin (Santa Cruz Biotechnology, SC-12732). Sections were incubated with their respective secondary antibodies diluted at 1:250 for 30min at room temperature. The slides were stained with 1:5000 dilution of DAPI for 5 min, mounted with Prolong Diamond Antifade Mountant (Invitrogen). To quantify the td-Tomato positive rate of myofibers, a sample of three sections for each animal was analyzed. Fluorescent images at × 60 magnification were taken using a confocal microscope system. Five random fields from each tissue section were imaged and the td-Tomato positive rate of myofibers was quantified. Fluorescent imaging was performed with either Zeiss Observer Z1 microscope or Nikon A1 confocal microscope.

4.7. Cytokine analysis

Fetal liver lysates were harvested and assessed for cytokine levels at 48 h post LNP1 injections. The freshly harvested fetal livers were lysed in Cell Lysis Buffer (Cell signaling technology) supplemented with 1% Protease Inhibitor Cocktail (Sigma-Aldrich). Total protein content in each sample was determined with the BCA protein assay kit (Thermo Fisher Scientific) per manufacturer's instructions. The cytokine levels were assessed using the Proinflammatory panel 1 (mouse) kit for MSD multi-spot assay system according to the manufacturer's instructions. Saline injection served as the control. Liver cytokine data were normalized to the total liver protein concentration, as determined by the BCA assay.

4.8. Statistic

Statistical analysis was performed by one-way analysis of variance (ANOVA) following Tukey's multiple comparison tests using PRISM 7 (GraphPad Software Inc., San Diego, CA, USA) for experiments involving the comparison of more than two groups. The flow cytometry characterized biodistribution and cytokine expression levels were analyzed by student's *t*-test. Statistical differences were considered significant if $p < 0.05$.

Ethics approval and consent to participate

All animal procedures were approved by the Institutional Animal Care and Use Committee at the University of California, Davis. Written informed consent was obtained from all participants.

CRediT authorship contribution statement

Kewa Gao: Conceptualization, Methodology, Data curation, Validation, Investigation, Formal analysis, Writing – original draft. **Jie Li:** Conceptualization, Methodology, Data curation, Validation, Investigation, Formal analysis, Writing – original draft. **Hengyue Song:** Methodology, Data curation, Investigation. **Hesong Han:** Methodology, Data curation, Investigation. **Yongheng Wang:** Methodology, Data curation, Investigation. **Boyan Yin:** Methodology, Data curation, Investigation. **Diana L. Farmer:** Writing – review & editing. **Niren Murthy:** Conceptualization, Funding acquisition, Project administration, Writing – review & editing. **Aijun Wang:** Conceptualization, Funding acquisition, Project administration, Writing – review & editing.

Declaration of competing interest

The authors declare no conflict of interest.

Acknowledgements

This work was in part supported by the California Institute for Regenerative Medicine (CIRM) grant DISC2-14097 (A.W.) and the National Institutes of Health grants UG3NS115599, R61DA048444–01, R01MH125979 (N.M.), 1R01NS100761 and 1R01NS115860 (A.W.).

Appendix A. Supplementary data

Supplementary data to this article can be found online at https://doi.org/10.1016/j.bioactmat.2023.02.011.

Supporting Information is available from the Wiley Online Library or from the author.

References

[1] H. Topaloglu, et al., Practice guideline update summary: corticosteroid treatment of Duchenne muscular dystrophy: report of the guideline development subcommittee of the American academy of neurology, Neurology 87 (2) (2016) 238.
[2] L. Romeiser Logan, K. Kolaski, Guideline to improve physical function in cerebral palsy: too big to succeed, Dev. Med. Child Neurol. 64 (5) (2022) 662–663.
[3] M. Mila, et al., [Clinical guideline of gene FMR1-associated diseases: fragile X syndrome, primary ovarian insufficiency and tremor-ataxia syndrome], Med. Clin. 142 (5) (2014) 219–225.
[4] A.C. Rossidis, et al., *In* utero CRISPR-mediated therapeutic editing of metabolic genes, Nat. Med. 24 (10) (2018) 1513–1518.
[5] D. Alapati, et al., *In* utero gene editing for monogenic lung disease, Sci. Transl. Med. 11 (488) (2019).
[6] Q.H. Nguyen, et al., Tolerance induction and microglial engraftment after fetal therapy without conditioning in mice with Mucopolysaccharidosis type VII, Sci. Transl. Med. 12 (532) (2020).
[7] L.M. Gan, et al., Intradermal delivery of modified mRNA encoding VEGF-A in patients with type 2 diabetes, Nat. Commun. 10 (1) (2019) 871.
[8] F. DeRosa, et al., Therapeutic efficacy in a hemophilia B model using a biosynthetic mRNA liver depot system, Gene Ther. 23 (10) (2016) 699–707.
[9] U. Sahin, K. Kariko, O. Tureci, mRNA-based therapeutics–developing a new class of drugs, Nat. Rev. Drug Discov. 13 (10) (2014) 759–780.
[10] S.K. Bose, P. Menon, W.H. Peranteau, InUtero gene therapy: progress and challenges, Trends Mol. Med. (2021).
[11] A.S. Ricciardi, et al., In utero nanoparticle delivery for site-specific genome editing, Nat. Commun. 9 (1) (2018) 2481.
[12] R.S. Riley, et al., Ionizable lipid nanoparticles for in utero mRNA delivery, Sci. Adv. 7 (3) (2021).
[13] M. Endo, et al., The developmental stage determines the distribution and duration of gene expression after early intra-amniotic gene transfer using lentiviral vectors, Gene Ther. 17 (1) (2010) 61–71.
[14] G. Massaro, et al., Fetal gene therapy for neurodegenerative disease of infants, Nat. Med. 24 (9) (2018) 1317–1323.

[15] S. Barua, S. Mitragotri, Challenges associated with penetration of nanoparticles across cell and tissue barriers: a review of current status and future prospects, Nano Today 9 (2) (2014) 223–243.
[16] S.A. Dilliard, Q. Cheng, D.J. Siegwart, On the mechanism of tissue-specific mRNA delivery by selective organ targeting nanoparticles, Proc. Natl. Acad. Sci. U. S. A. 118 (52) (2021).
[17] J.A. Kulkarni, P.R. Cullis, R. van der Meel, Lipid nanoparticles enabling gene therapies: from concepts to clinical utility, Nucleic Acid Therapeut. 28 (3) (2018) 146–157.
[18] A. Nijagal, et al., A mouse model of in utero transplantation, JoVE (47) (2011).
[19] M.M. Boelig, et al., The intravenous route of injection optimizes engraftment and survival in the murine model of in utero hematopoietic cell transplantation, Biol. Blood Marrow Transplant. 22 (6) (2016) 991–999.
[20] N.J. Ahn, et al., Intravenous and intra-amniotic in utero transplantation in the murine model, JoVE 140 (2018).
[21] B.F. Haynes, A new vaccine to battle covid-19, N. Engl. J. Med. 384 (5) (2021) 470–471.
[22] K. Garber, Alnylam launches era of RNAi drugs, Nat. Biotechnol. 36 (9) (2018) 777–778.
[23] Q. Cheng, et al., Selective organ targeting (SORT) nanoparticles for tissue-specific mRNA delivery and CRISPR-Cas gene editing, Nat. Nanotechnol. 15 (4) (2020) 313–320.
[24] K.T. Love, et al., Lipid-like materials for low-dose, in vivo gene silencing, Proc. Natl. Acad. Sci. U. S. A. 107 (5) (2010) 1864–1869.
[25] T.M. Allen, P.R. Cullis, Liposomal drug delivery systems: from concept to clinical applications, Adv. Drug Deliv. Rev. 65 (1) (2013) 36–48.
[26] I.S. Zuhorn, et al., Nonbilayer phase of lipoplex-membrane mixture determines endosomal escape of genetic cargo and transfection efficiency, Mol. Ther. 11 (5) (2005) 801–810.
[27] M.A. Oberli, et al., Lipid nanoparticle assisted mRNA delivery for potent cancer immunotherapy, Nano Lett. 17 (3) (2017) 1326–1335.
[28] C. Walsh, et al., Microfluidic-based manufacture of siRNA-lipid nanoparticles for therapeutic applications, Methods Mol. Biol. 1141 (2014) 109–120.
[29] E.M. Otis, R. Brent, Equivalent ages in mouse and human embryos, Anat. Rec. 120 (1) (1954) 33–63.
[30] S. Goenezen, M.Y. Rennie, S. Rugonyi, Biomechanics of early cardiac development, Biomech. Model. Mechanobiol. 11 (8) (2012) 1187–1204.
[31] J.R. Walls, et al., Three-dimensional analysis of vascular development in the mouse embryo, PLoS One 3 (8) (2008) e2853.
[32] D. Witzigmann, et al., Lipid nanoparticle technology for therapeutic gene regulation in the liver, Adv. Drug Deliv. Rev. 159 (2020) 344–363.
[33] G. Hoeffel, F. Ginhoux, Fetal monocytes and the origins of tissue-resident macrophages, Cell. Immunol. 330 (2018) 5–15.
[34] K.A. Hajj, K.A. Whitehead, Tools for translation: non-viral materials for therapeutic mRNA delivery, Nat. Rev. Mater. 2 (10) (2017) 1–17.
[35] W.M. Pardridge, Blood-brain barrier and delivery of protein and gene therapeutics to brain, Front. Aging Neurosci. 11 (2019) 373.
[36] N.R. Saunders, et al., The rights and wrongs of blood-brain barrier permeability studies: a walk through 100 years of history, Front. Neurosci. 8 (2014) 404.
[37] A. Ben-Zvi, et al., Mfsd2a is critical for the formation and function of the blood-brain barrier, Nature 509 (7501) (2014) 507–+.
[38] L. Kassar-Duchossoy, et al., Pax3/Pax7 mark a novel population of primitive myogenic cells during development, Genes Dev. 19 (12) (2005) 1426–1431.
[39] N. Nicolas, C.L. Gallien, C. Chanoine, Expression of myogenic regulatory factors during muscle development of Xenopus: myogenin mRNA accumulation is limited strictly to secondary myogenesis, Dev. Dynam. 213 (3) (1998) 309–321.
[40] J.E. Dahlman, et al., In vivo endothelial siRNA delivery using polymeric nanoparticles with low molecular weight, Nat. Nanotechnol. 9 (8) (2014) 648–655.
[41] J.R. Sanes, Laminin, fibronectin, and collagen in synaptic and extrasynaptic portions of muscle fiber basement membrane, J. Cell Biol. 93 (2) (1982) 442–451.
[42] A.C. Chadwick, X. Wang, K. Musunuru, *In* vivo base editing of PCSK9 (proprotein convertase subtilisin/kexin type 9) as a therapeutic alternative to genome editing, Arterioscler. Thromb. Vasc. Biol. 37 (9) (2017) 1741–+.
[43] A.C. Rossidis, et al., *In* utero CRISPR-mediated therapeutic editing of metabolic genes, Nat. Med. 24 (10) (2018) 1513–+.
[44] N.K. Paulk, et al., Adeno-associated virus gene repair corrects a mouse model of hereditary tyrosinemia in vivo, Hepatology 51 (4) (2010) 1200–1208.
[45] A. Hendel, et al., Chemically modified guide RNAs enhance CRISPR-Cas genome editing in human primary cells, Nat. Biotechnol. 33 (9) (2015), 985-U232.
[46] H. Yin, et al., Structure-guided chemical modification of guide RNA enables potent non-viral in vivo genome editing, Nat. Biotechnol. 35 (12) (2017) 1179–+.
[47] S. Riesenberg, et al., Improved gRNA secondary structures allow editing of target sites resistant to CRISPR-Cas9 cleavage, Nat. Commun. 13 (1) (2022).
[48] P. Kumar, et al., *In* utero transplantation of placenta-derived mesenchymal stromal cells for potential fetal treatment of hemophilia A, Cell Transplant. 27 (1) (2018) 130–139.
[49] K. Gao, et al., Clonal isolation of endothelial colony-forming cells from early gestation chorionic villi of human placenta for fetal tissue regeneration, World J. Stem Cell. 12 (2) (2020) 123–138.
[50] L. Lankford, et al., Early gestation chorionic villi-derived stromal cells for fetal tissue engineering, World J. Stem Cell. 7 (1) (2015) 195–207.